

# Scalable Spectral-Geometric-Algebraic Multigrid and Schur Complement Preconditioning for Nonlinear, Multiscale, Heterogeneous Flow in Earth's Mantle

Johann Rudi

Institute for Computational Engineering and Sciences,  
The University of Texas at Austin, USA

Co-Advisors

Omar Ghattas (UT Austin) and Georg Stadler (New York University)

Collaborators

Tobin Isaac (U Chicago), Michael Gurnis (Caltech), and from IBM Research – Zurich: Cristiano I. Malossi, Peter W.J. Staar, Yves Ineichen, Costas Bekas, Alessandro Curioni

## Outline

Earth’s mantle convection: Driving application & solver challenges

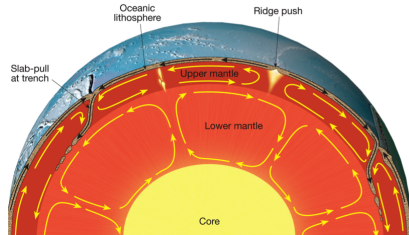
Preconditioner for the inverse Schur complement: Weighted BFBT

Preconditioning with Hybrid Spectral–Geometric–Algebraic Multigrid

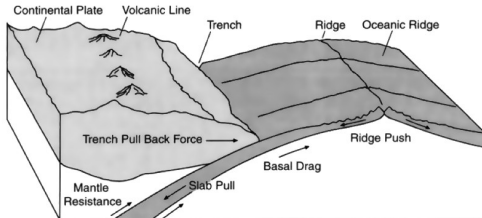
Numerical results: Algorithmic & parallel scalability

## Mantle convection & plate tectonics

- ▶ Mantle convection is the thermal convection in earth’s upper  $\sim 3000$  km
- ▶ It controls the thermal and geological evolution of the Earth
- ▶ Solid rock in the mantle moves like viscous incompressible fluid on time scales of millions of years
- ▶ Driver for plate tectonics, earthquakes, tsunamis, volcanos



Convection layering (Credit: Pearson Prentice Hall, Inc.)



Subducting slab (Credit: Schubert, Turcotte, Olsen)

- ▶ Main drivers of plate motion: negative buoyancy forces or convective shear traction?
- ▶ Key process governing the occurrence of great earthquakes: material properties between the plates or tectonic stress?

## What we know: Observational data

- ▶ Current **plate motion** from GPS and magnetic anomalies
- ▶ **Plate deformation** obtained from dense GPS networks
- ▶ **Average viscosity** in regions affected by post-glacial rebound
- ▶ **Topography** indicating normal traction at earth’s surface

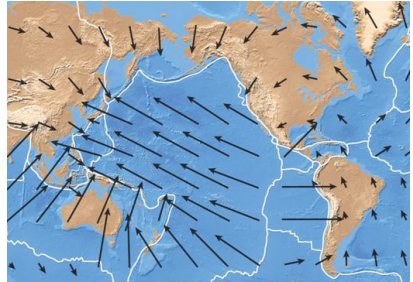


Plate motion (Credit: Pearson Prentice Hall, Inc.)

Additional knowledge contributing to mantle rheology:

- ▶ Location and geometry of plates, **plate boundaries**, and subducting slabs (from seismicity)
- ▶ **Rock rheology** extrapolated from laboratory experiments
- ▶ Images of present-day **earth structure** (by correlating seismic wave speed with temperature)

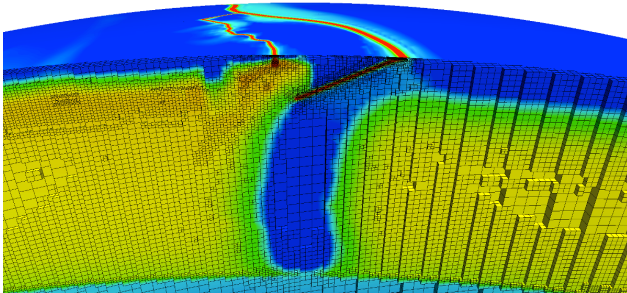
## What we would like to learn: Rheological parameters

Globally constant parameters affecting viscosity and nonlinearity:

- ▶ **Scaling factor** of the upper mantle viscosity (down to  $\sim 660$  km depth)
- ▶ **Stress exponent** controlling severity of strain rate weakening
- ▶ **Yield strength** governing plastic yielding phenomena

Local, spatially varying parameters:

- ▶ **Coupling strength** / energy dissipation between plates



## Mantle flow governed by incompressible Stokes equations

Nonlinear incompressible Stokes PDE (w/ free-slip & no-normal flow BC):

$$\begin{aligned} -\nabla \cdot [\mu(\mathbf{u}) (\nabla \mathbf{u} + \nabla \mathbf{u}^T)] + \nabla p &= \mathbf{f} && \text{viscosity } \mu, \text{ RHS forcing } \mathbf{f} \\ -\nabla \cdot \mathbf{u} &= 0 && \text{seek: velocity } \mathbf{u}, \text{ pressure } p \end{aligned}$$

Linearization (with Newton), then discretization (with inf-sup stable F.E.):

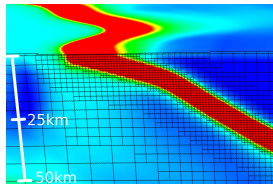
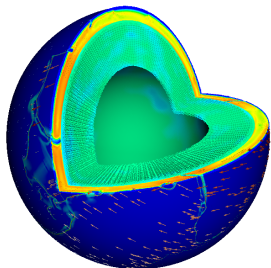
$$\begin{bmatrix} \mathbf{A} & \mathbf{B}^T \\ \mathbf{B} & \mathbf{0} \end{bmatrix} \begin{bmatrix} \tilde{\mathbf{u}} \\ \tilde{\mathbf{p}} \end{bmatrix} = \begin{bmatrix} -\mathbf{r}_1 \\ -\mathbf{r}_2 \end{bmatrix}$$

- ▶ **High-order** finite element shape functions
- ▶ Inf-sup **stable velocity–pressure pairings**:  $\mathbb{Q}_k \times \mathbb{P}_{k-1}^{\text{disc}}$  with order  $k \geq 2$
- ▶ **Locally mass conservative** due to discontinuous, modal pressure
- ▶ **Adaptive mesh refinement** resolving fine-scale features of mantle
- ▶ **Non-conforming** hexahedral meshes with “hanging nodes”

## Severe challenges for parallel scalable solvers

... arising in Earth’s mantle convection:

- ▶ Severe **nonlinearity, heterogeneity, and anisotropy** due to Earth’s rheology (strain rate weakening, plastic yielding)
- ▶ **Sharp viscosity gradients** in narrow regions (6 orders of magnitude drop in  $\sim 5$  km)
- ▶ **Wide range of spatial scales and highly localized features**, e.g., plate boundaries of size  $\mathcal{O}(1$  km) influence plate motion at continental scales of  $\mathcal{O}(1000$  km)
- ▶ **Adaptive mesh refinement** is essential
- ▶ **High-order** finite elements  $\mathbb{Q}_k \times \mathbb{P}_{k-1}^{\text{disc}}$ , order  $k \geq 2$ , with **local mass conservation**; yields a difficult to deal with **discontinuous, modal pressure** approximation



Viscosity (colors) and locally refined mesh.

## Outline

Earth's mantle convection: Driving application & solver challenges

Preconditioner for the inverse Schur complement: Weighted BFBT

Preconditioning with Hybrid Spectral–Geometric–Algebraic Multigrid

Numerical results: Algorithmic & parallel scalability



## Preconditioning of saddle-point systems from PDEs

Iterative scheme with upper triangular block preconditioning:

$$\begin{bmatrix} \mathbf{A} & \mathbf{B}^T \\ \mathbf{B} & \mathbf{0} \end{bmatrix} \begin{bmatrix} \tilde{\mathbf{A}} & \mathbf{B}^T \\ \mathbf{0} & \tilde{\mathbf{S}} \end{bmatrix}^{-1} \begin{bmatrix} \tilde{\mathbf{u}} \\ \tilde{\mathbf{p}} \end{bmatrix} = \begin{bmatrix} -\mathbf{r}_1 \\ -\mathbf{r}_2 \end{bmatrix} \quad \begin{array}{l} \tilde{\mathbf{A}}^{-1} \approx \mathbf{A}^{-1} \\ \tilde{\mathbf{S}}^{-1} \approx \mathbf{S}^{-1} := (\mathbf{B}\mathbf{A}^{-1}\mathbf{B}^T)^{-1} \end{array}$$

Commonly occurring preconditioning challenge in CS&E:

- ▶ Creeping non-Newtonian fluid modeled by incompressible Stokes equations with power-law rheology yields **spatially-varying and highly heterogeneous** viscosity  $\mu$  after linearization.

## Preconditioning of saddle-point systems from PDEs

Iterative scheme with upper triangular block preconditioning:

$$\begin{bmatrix} \mathbf{A} & \mathbf{B}^T \\ \mathbf{B} & \mathbf{0} \end{bmatrix} \begin{bmatrix} \tilde{\mathbf{A}} & \mathbf{B}^T \\ \mathbf{0} & \tilde{\mathbf{S}} \end{bmatrix}^{-1} \begin{bmatrix} \tilde{\mathbf{u}} \\ \tilde{\mathbf{p}} \end{bmatrix} = \begin{bmatrix} -\mathbf{r}_1 \\ -\mathbf{r}_2 \end{bmatrix} \quad \begin{array}{l} \tilde{\mathbf{A}}^{-1} \approx \mathbf{A}^{-1} \\ \tilde{\mathbf{S}}^{-1} \approx \mathbf{S}^{-1} := (\mathbf{B}\mathbf{A}^{-1}\mathbf{B}^T)^{-1} \end{array}$$

Commonly occurring preconditioning challenge in CS&E:

- ▶ Creeping non-Newtonian fluid modeled by incompressible Stokes equations with power-law rheology yields **spatially-varying and highly heterogeneous** viscosity  $\mu$  after linearization.

Possible preconditioners for the **inverse Schur complement**  $\mathbf{S}^{-1}$ :

- ▶ Viscosity-weighted pressure mass matrix,  $\mathbf{M}_p(1/\mu)$ : [Burstedde, Ghattas, Stadler, et al., 2009], [Grinevich and Olshanskii, 2009]
- ▶ BFBT for Navier–Stokes: [Elman, 1999], [Silvester, Elman, Kay, Wathen, 2001], [Kay, Loghin, Wathen, 2002], [Elman, Tuminaro, 2009]
- ▶ BFBT for variable-viscosity Stokes: [May, Moresi, 2008]

## Weighted BFBT: Inverse Schur complement approximation

$$\begin{bmatrix} \mathbf{A} & \mathbf{B}^\top \\ \mathbf{B} & \mathbf{0} \end{bmatrix} \begin{bmatrix} \tilde{\mathbf{A}} & \mathbf{B}^\top \\ \mathbf{0} & \tilde{\mathbf{S}} \end{bmatrix}^{-1} \begin{bmatrix} \tilde{\mathbf{u}} \\ \tilde{\mathbf{p}} \end{bmatrix} = \begin{bmatrix} -\mathbf{r}_1 \\ -\mathbf{r}_2 \end{bmatrix} \quad \begin{aligned} \tilde{\mathbf{A}}^{-1} &\approx \mathbf{A}^{-1} \\ \tilde{\mathbf{S}}^{-1} &\approx (\mathbf{B}\mathbf{A}^{-1}\mathbf{B}^\top)^{-1} \end{aligned}$$

## Weighted BFBT: Inverse Schur complement approximation

$$\begin{bmatrix} \mathbf{A} & \mathbf{B}^\top \\ \mathbf{B} & \mathbf{0} \end{bmatrix} \begin{bmatrix} \tilde{\mathbf{A}} & \mathbf{B}^\top \\ \mathbf{0} & \tilde{\mathbf{S}} \end{bmatrix}^{-1} \begin{bmatrix} \tilde{\mathbf{u}} \\ \tilde{\mathbf{p}} \end{bmatrix} = \begin{bmatrix} -\mathbf{r}_1 \\ -\mathbf{r}_2 \end{bmatrix} \quad \begin{aligned} \tilde{\mathbf{A}}^{-1} &\approx \mathbf{A}^{-1} \\ \tilde{\mathbf{S}}^{-1} &\approx (\mathbf{B}\mathbf{A}^{-1}\mathbf{B}^\top)^{-1} \end{aligned}$$

From a “commutator relationship” leading to a least-squares minimization problem, we derive the BFBT approximation:

$$\tilde{\mathbf{S}}_{w\text{-BFBT}}^{-1} := \underbrace{(\mathbf{B}\mathbf{C}_w^{-1}\mathbf{B}^\top)^{-1}}_{\text{Poisson solve}} (\mathbf{B}\mathbf{C}_w^{-1}\mathbf{A}\mathbf{D}_w^{-1}\mathbf{B}^\top) \underbrace{(\mathbf{B}\mathbf{D}_w^{-1}\mathbf{B}^\top)^{-1}}_{\text{Poisson solve}}$$

## Weighted BFBT: Inverse Schur complement approximation

$$\begin{bmatrix} \mathbf{A} & \mathbf{B}^\top \\ \mathbf{B} & \mathbf{0} \end{bmatrix} \begin{bmatrix} \tilde{\mathbf{A}} & \mathbf{B}^\top \\ \mathbf{0} & \tilde{\mathbf{S}} \end{bmatrix}^{-1} \begin{bmatrix} \tilde{\mathbf{u}} \\ \tilde{\mathbf{p}} \end{bmatrix} = \begin{bmatrix} -\mathbf{r}_1 \\ -\mathbf{r}_2 \end{bmatrix} \quad \begin{array}{l} \tilde{\mathbf{A}}^{-1} \approx \mathbf{A}^{-1} \rightarrow \text{MG V-cycle} \\ \tilde{\mathbf{S}}^{-1} \approx (\mathbf{B}\mathbf{A}^{-1}\mathbf{B}^\top)^{-1} \end{array}$$

From a “commutator relationship” leading to a least-squares minimization problem, we derive the BFBT approximation:

$$\tilde{\mathbf{S}}_{w\text{-BFBT}}^{-1} := \underbrace{(\mathbf{B}\mathbf{C}_w^{-1}\mathbf{B}^\top)^{-1}}_{\rightarrow \text{MG V-cycle}} (\mathbf{B}\mathbf{C}_w^{-1}\mathbf{A}\mathbf{D}_w^{-1}\mathbf{B}^\top) \underbrace{(\mathbf{B}\mathbf{D}_w^{-1}\mathbf{B}^\top)^{-1}}_{\rightarrow \text{MG V-cycle}}$$

Choice of diagonal weighting matrices  $\mathbf{C}_w$ ,  $\mathbf{D}_w$  is critical for efficacy & robustness with respect to viscosity variations.

- ▶ [May, Moresi, 2008] introduces  $\mathbf{C}_w$ ,  $\mathbf{D}_w$  based on entries of  $\mathbf{A}$
- ▶ [Rudi, Malossi, Isaac, et al., 2015] uses  $\mathbf{C}_w = \mathbf{D}_w := \text{diag}(\mathbf{A})$
- ▶ [Rudi, Stadler, Ghattas, 2017] proposes  $\mathbf{C}_w = \mathbf{D}_w := \tilde{\mathbf{M}}_u(\sqrt{\mu})$

## Benchmark problem: Multiple sinkers at random locations

Two parameters increase problem difficulty:

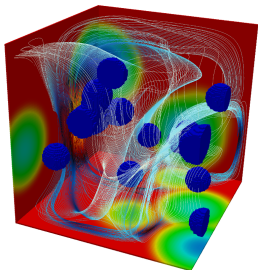
- ▶ **Number of sinkers**  $n$  at **random** points  $\mathbf{c}_i$
- ▶ **Dynamic ratio**  $\text{DR}(\mu) := \mu_{\max}/\mu_{\min}$

Smooth but highly varying viscosity  $\mu$  is defined as:

$$\mu(\mathbf{x}) := (\mu_{\max} - \mu_{\min})(1 - \chi_n(\mathbf{x})) + \mu_{\min}$$

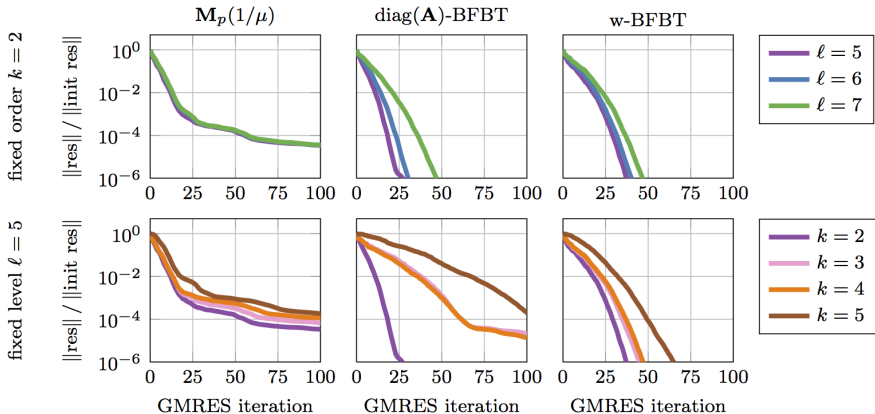
$$\chi_n(\mathbf{x}) := \prod_{i=1}^n 1 - \exp \left[ -d \max \left( 0, |\mathbf{c}_i - \mathbf{x}| - \frac{w}{2} \right)^2 \right]$$

(where  $\mu_{\min}, \mu_{\max}, d, w$  are constant)



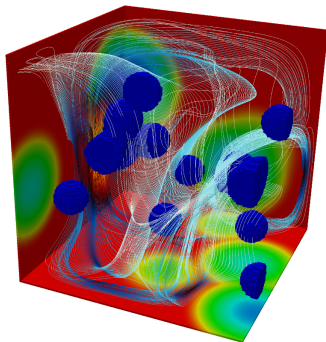
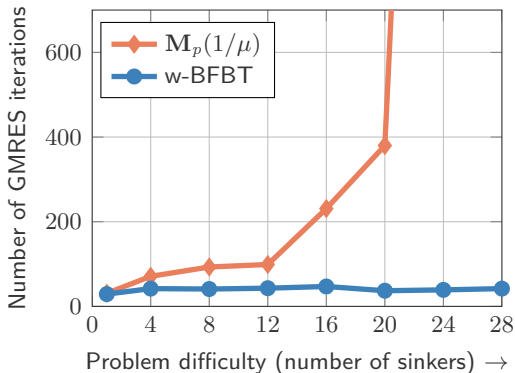
Smooth viscosity (colors) with highest value (blue) assumed inside spheres; streamlines show velocity field.

## Comparison of Schur complement preconditioners



- ▶ Convergence of GMRES for benchmark problem with challenging viscosity  $\mu$
- ▶  $k$  is velocity discretization order and  $\ell$  is refinement level of uniform mesh
- ▶  $w\text{-BFBT}$ , where  $\mathbf{C}_w = \mathbf{D}_w := \tilde{\mathbf{M}}_u(\sqrt{\mu})$ , combines robust convergence of  $\text{diag}(\mathbf{A})\text{-BFBT}$  with improved algorithmic scalability when order  $k$  increases

## Robustness of w-BFBT w.r.t. viscosity variations



- ▶ Graph shows excerpt from more extensive numerical study
- ▶ Preconditioner  $M_p(1/\mu)$  becomes ineffective as sinker count increases
- ▶ w-BFBT is largely unaffected by viscosity variations, which makes it advantageous for highly heterogeneous problems



## Spectral equivalence for w-BFBT

**Theorem:** [Rudi, Stadler, Ghattas, 2017] Assume an infinite-dimensional w-BFBT approximation of the Schur complement:

$$\tilde{S}_{w\text{-BFBT}} := K_w^* (Bw A wB^*)^{-1} K_w, \quad K_w^* := BwB^*, \quad w \equiv \mu^{-\frac{1}{2}}$$

Then  $\tilde{S}_{w\text{-BFBT}}$  is equivalent to  $S = BA^{-1}B^*$ ,

$$\left( \tilde{S}_{w\text{-BFBT}} q, q \right) \leq (Sq, q) \leq C_{w\text{-BFBT}} \left( \tilde{S}_{w\text{-BFBT}} q, q \right) \quad \text{for all } q,$$

with a constant based on weighted Poincaré–Friedrichs’ and Korn’s ineq.

$$C_{w\text{-BFBT}} := \left( 1 + \frac{1}{4} \|\nabla\mu\|_{L^\infty(\Omega)^d}^2 \right) \left( C_{P,\mu}^2 + 1 \right) C_{K,\mu}^2$$

**Remark:** For a constant viscosity  $\mu \equiv 1$  the equivalence relationship holds with classical Poincaré–Friedrichs’ and Korn’s inequalities.

## Proof idea (Spectral equivalence for w-BFBT)

1. Establish a “sup-form” for approx. and exact Schur complements:

$$\begin{aligned} \left( \tilde{S}_{w\text{-BFBT}} q, q \right) &= \sup_p \frac{(B^* p, wB^* q)^2}{(wAwB^* p, B^* p)} \\ (Sq, q) &= \sup_v \frac{(\mathbf{v}, wB^* q)^2}{(wAw\mathbf{v}, \mathbf{v})} \end{aligned}$$

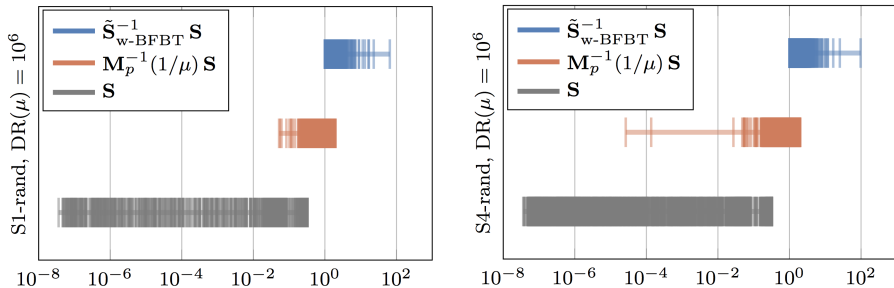
2. Lower estimate (with constant one) follows immediately.
3. For the upper estimate, derive that

$$\begin{aligned} \frac{1}{2C_{\mu,w}} \|wB^* q\|_{(H^{-1}(\Omega))^d}^2 &\leq \left( \tilde{S}_{w\text{-BFBT}} q, q \right), \\ (Sq, q) &\leq \sup_v \frac{\|w^{-1}\mathbf{v}\|_{(H^1(\Omega))^d}^2 \|wB^* q\|_{(H^{-1}(\Omega))^d}^2}{2 \left\| \sqrt{\mu} \frac{1}{2} (\nabla \mathbf{v} + \nabla \mathbf{v}^T) \right\|_{(L^2(\Omega))^{d \times d}}^2}. \end{aligned}$$

Result follows with weighted Poincaré–Friedrichs’ and Korn’s ineq.

## Spectrum comparisons of preconditioned Schur matrices

2D Stokes problem discretized with  $\mathbb{P}_2^{\text{bubble}} \times \mathbb{P}_1^{\text{disc}}$  elements (FEniCS library)



- ▶ As the problem difficulty (i.e., sinker counts) increases, the spreading of small eigenvalues for  $\mathbf{M}_p(1/\mu)$  becomes more severe, which is disadvantageous for Krylov solver convergence.
- ▶ w-BFBT remains largely unaffected by increased difficulty, which results in convergence that is robust with respect to viscosity variations.

## Outline

Earth's mantle convection: Driving application & solver challenges

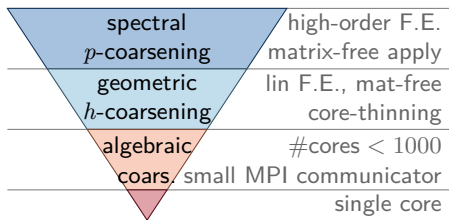
Preconditioner for the inverse Schur complement: Weighted BFBT

Preconditioning with Hybrid Spectral–Geometric–Algebraic Multigrid

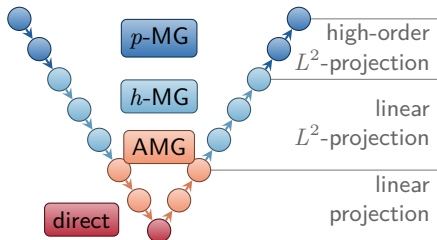
Numerical results: Algorithmic & parallel scalability

# HMG: Hybrid spectral–geometric–algebraic multigrid

## HMG hierarchy



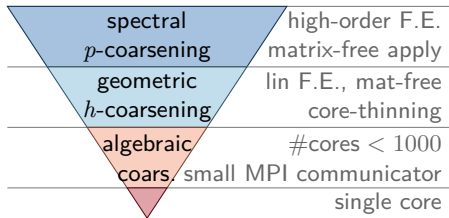
## HMG V-cycle



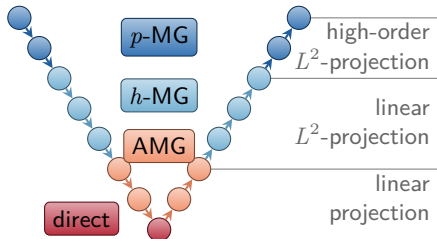
- ▶ Multigrid hierarchy of nested meshes is generated from an **adaptively refined octree-based mesh** via spectral–geometric coarsening
- ▶ **Re-discretization** of PDEs at coarser levels
- ▶ **Parallel repartitioning** of coarser meshes for load-balancing (crucial for AMR); sufficiently coarse meshes occupy only **subsets of cores**
- ▶ **Coarse grid solver**: AMG (from PETSc) invoked on small core counts

# HMG: Hybrid spectral–geometric–algebraic multigrid

HMG hierarchy

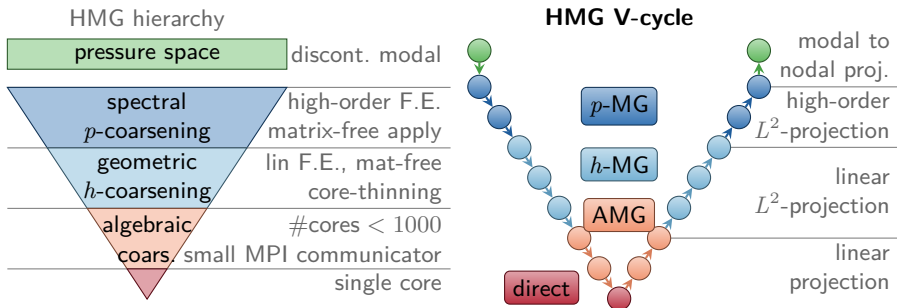


HMG V-cycle



- ▶ High-order  $L^2$ -projection onto coarser levels; restriction & interpolation are adjoints of each other in  $L^2$ -sense
- ▶ Chebyshev accelerated Jacobi smoother (Cheb. from PETSc) with tensorized matrix-free high-order stiffness apply; assembly of high-order diagonal only
- ▶ Efficacy, i.e., error reduction, of HMG V-cycles is independent of core count
- ▶ No collective communication needed in spectral–geometric MG cycles

## HMG: Hybrid spectral–geometric–algebraic multigrid

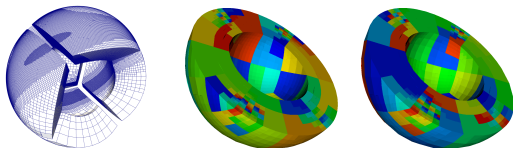
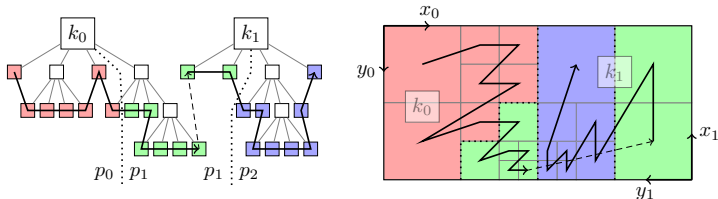


- ▶ **High-order  $L^2$ -projection** onto coarser levels; restriction & interpolation are adjoints of each other in  $L^2$ -sense
- ▶ **Chebyshev accelerated Jacobi smoother** (Cheb. from PETSc) with tensorized matrix-free high-order stiffness apply; assembly of high-order diagonal only
- ▶ Efficacy, i.e., error reduction, of HMG V-cycles is **independent of core count**
- ▶ **No collective communication** needed in spectral–geometric MG cycles

## p4est: Parallel forest-of-octrees AMR library [p4est.org]

Scalable geometric multigrid coarsening due to:

- ▶ **Forest-of-octree** based meshes enable fast refinement/coarsening
- ▶ Octrees and **space filling curves** used for fast neighbor search, mesh repartitioning, and 2:1 mesh balancing in parallel

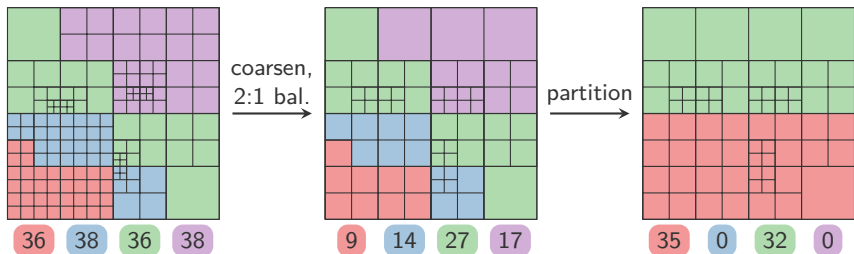


Colors depict different processor cores. (Credit: Burstedde, et al.)



## Geometric coarsening: Repartitioning & core-thinning

- ▶ Parallel repartitioning of locally refined meshes for **load balancing**
- ▶ **Core-thinning** to avoid excessive communication in multigrid cycle
- ▶ **Reduced MPI communicators** containing only non-empty cores
- ▶ **Ensure coarsening across core boundaries**: Partition families of octants/elements on same core for next coarsening sweep



Colors depict different processor cores, numbers indicate element count on each core.

[Sundar, Biros, Burstedde, Rudi, Ghattas, Stadler, 2012]

# Outline

Earth's mantle convection: Driving application & solver challenges

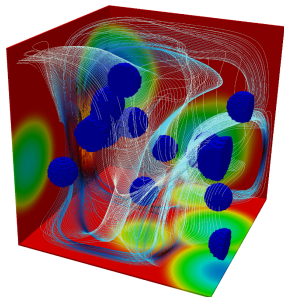
Preconditioner for the inverse Schur complement: Weighted BFBT

Preconditioning with Hybrid Spectral–Geometric–Algebraic Multigrid

Numerical results: Algorithmic & parallel scalability

## Algorithmic scalability for HMG+w-BFBT

Number of iterations for solving elliptic sub-systems  $\mathbf{A}\mathbf{u} = \mathbf{f}$ ,  $(\mathbf{B}\mathbf{D}_w^{-1}\mathbf{B}^T)\mathbf{p} = \mathbf{K}\mathbf{p} = \mathbf{g}$ , and full Stokes system for benchmark sinker problem.



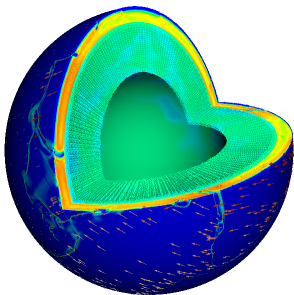
Vary mesh refinement  $\ell$  for fixed order  $k = 2$

| $\ell$ | $u$ -DOF<br>[ $\times 10^6$ ] | It. <b>A</b> | $p$ -DOF<br>[ $\times 10^6$ ] | It. <b>K</b> | DOF<br>[ $\times 10^6$ ] | It. <b>Stokes</b> |
|--------|-------------------------------|--------------|-------------------------------|--------------|--------------------------|-------------------|
| 4      | 0.11                          | 18           | 0.02                          | 8            | 0.12                     | 40                |
| 5      | 0.82                          | 18           | 0.13                          | 7            | 0.95                     | 33                |
| 6      | 6.44                          | 18           | 1.05                          | 6            | 7.49                     | 33                |
| 8      | 405.02                        | 18           | 67.11                         | 6            | 472.12                   | 34                |
| 10     | 25807.57                      | 18           | 4294.97                       | 6            | 30102.53                 | 34                |

Vary order  $k$  for fixed mesh refinement  $\ell = 5$

| $k$ | $u$ -DOF<br>[ $\times 10^6$ ] | It. <b>A</b> | $p$ -DOF<br>[ $\times 10^6$ ] | It. <b>K</b> | DOF<br>[ $\times 10^6$ ] | It. <b>Stokes</b> |
|-----|-------------------------------|--------------|-------------------------------|--------------|--------------------------|-------------------|
| 2   | 0.82                          | 18           | 0.13                          | 7            | 0.95                     | 33                |
| 3   | 2.74                          | 20           | 0.32                          | 8            | 3.07                     | 37                |
| 4   | 6.44                          | 20           | 0.66                          | 7            | 7.10                     | 36                |
| 6   | 21.56                         | 23           | 1.84                          | 12           | 23.40                    | 50                |
| 8   | 50.92                         | 22           | 3.93                          | 10           | 54.86                    | 67                |

## Parallel scalability: Global mantle convection problem setup



Discretization parameters to test parallel scalability:

- ▶ Finite element order  $k = 2$  is fixed ( $\mathbb{Q}_k \times \mathbb{P}_{k-1}^{\text{disc}}$ )
- ▶ Increase max mesh refinement  $\ell_{\max}$
- ▶ Refinement down to  $\sim 75$  m local resolution
- ▶ Resulting mesh has 9 levels of refinement

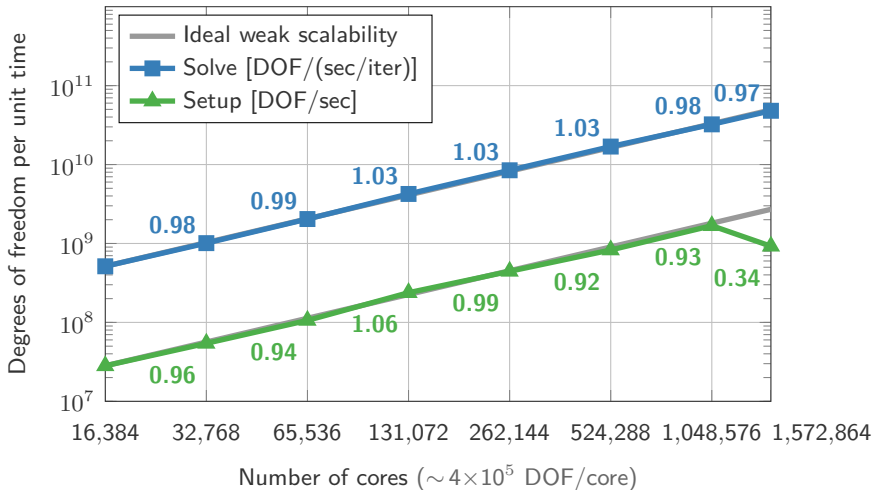
Multigrid parameters for elliptic blocks  $\mathbf{A}$  and  $\mathbf{K}$ :

- ▶ 1 HMG V-cycle with 3+3 smoothing

Hardware and target system:

- ▶ IBM Blue Gene/Q architecture
- ▶ Lawrence Livermore National Lab's Sequoia
- ▶ 96 racks resulting in 98,304 nodes and 1,572,864 cores

## Extreme weak scalability on Sequoia supercomputer



## Summary & References

### Summary of results:

- ▶ Weighted BFBT preconditioner for the for the Schur complement; scalable HMG-based BFBT algorithms, heterogeneity-robust weighting of BFBT and theoretical foundation.
- ▶ Hybrid spectral–geometric–algebraic multigrid; based on p4est library.
- ▶ Optimal or nearly optimal algorithmic scalability.
- ▶ Parallel scalability of solvers to 1.6 million cores.

---

### References:

- ▶ Rudi, Stadler, Ghattas, SIAM J. Sci. Comput.(2017), to appear.
- ▶ Rudi, Malossi, Isaac, Stadler, Gurnis, Ineichen, Bekas, Curioni, and Ghattas, Proceedings of SC15 (2015), Gordon Bell Prize.
- ▶ Sundar, Biros, Burstedde, Rudi, Ghattas, and Stadler, Proceedings of SC12 (2012).